

BONDGRAPHS MODELING AND SIMULATION ON DYNAMIC CHARACTERISTICS OF CAVITATING PUMP SYSTEM

Kazuhiro TANAKA^(a), Toshiyuki SATO^(b), Hiroshi TSUKAMOTO^(c), Takehisa KOHDA^(d), Katsuya SUZUKI^(e)

^{(a)(e)}Dept. of Mech. Information Science and Technology, Kyushu Institute of Technology, Iizuka 820-8502, Japan

^(b)Hitachi Ltd., Infrastructure Systems Company, Tsuchiura 300-0013, Japan

^(c)Kitakyushu National College of Japan, Kitakyushu 802-0985, Japan

^(b)Dept. of Aeronautics and Astronautics, Kyoto University, Kyoto 606-8501, Japan

^(a)kazuhiro@mse.kyutech.ac.jp, ^(b)toshiyuki.sato.bh@hitachi.com, ^(e)htsuka@kct.ac.jp,

^(d)kohda.takehisa.5m@kyoto-u.ac.jp, ^(e)kachandesu2002@yahoo.co.jp

ABSTRACT

Internal flows including cavitation phenomena in a pump can be analyzed by CFD commercial codes and system performances are traditionally obtained by experimental tests. However, they cannot correctly analyze the dynamic characteristics of the system especially when the transients are very fast or the system sometimes becomes complicated according to cavitation phenomena. It is important to predict dynamic behaviors of the pump system in the development stage. 3D-CFD numerical calculation is so time-consuming to analyze total flow field in the system that it is useful to develop 1D-mathematical models to express the dynamic characteristics of the system. The mathematical models of a pump system already have been developed by Bondgraphs without cavitation phenomena. In this study, the numerical result of cavitating flow is considered into the system Bondgraphs.

Keywords: pump system dynamics, Bondgraphs, CFD result, cavitating flow

NOMENCLATURE

B: flow passage width in the impeller
 c: radial velocity of fluid in velocity triangle
 C_{cav} : element representing cavitation
 C_p : cavitation compliance
 D: diameter
 d: pipe diameter
 f_0 : cavitation surging frequency
 H_{sv} : net positive suction head
 I : inertia of rotational parts of pump, $I = I_m + I_s + I_l$
 I_l : rotational inertia of liquid within the impeller
 I_q : fluid inertia of liquid in the pipe
 I_{q1} : fluid inertia in suction pipe
 I_w : through flow inertia of liquid within the impeller
 K: bulk modulus
 L: length of flow passage of whole system
 M_b : mass flow gain factor
 P, ΔP : pressure, pressure difference
 Q: flow rate, discharge
 Q_0 : rated flow rate

R: impeller radius
 R_c : contraction loss in Rc element
 R_e : expansion loss in Re element
 R_g : power gyrating parameter in MGY element
 R_l : leakage loss in Rl element
 R_{pf} : pipe friction parameter
 R_{if}, R_{is} : losses in an impeller in Rif and Ris elements
 R_s : flow resistance in suction pipe
 R_v : hydraulic loss parameter in a valve, in Rv element
 R_{vf}, R_{vs} : losses in a volute in Rvf and Rvs elements
 R_w : disk loss parameter in R ω element
 T, ΔT : torque, torque loss
 t: time
 U: fluid velocity
 u: peripheral velocity of an impeller
 V: absolute velocity
 v: absolute velocity of an impeller in velocity triangle
 V_c : cavitation volume
 W: relative velocity of fluid within the impeller in velocity triangle
 Z: number of blades of the impeller
 α : angle between u and c in the velocity triangle, void fraction
 β_2 : flow angle with the slip factor at the impeller outlet
 β_{b2} : blade angle at the impeller outlet
 φ : flow coefficient = $\overline{Q_2} / (B_2 u_2)$
 ρ : density
 σ : cavitation number = $H_{sv} / (u_1^2 / 2g)$
 τ : shear stress
 ω : rotational speed

Subscript:

0: rated value
 1: inlet of impeller, suction side
 2: outlet of impeller, delivery side
 I, i: impeller
 m: motor
 s: shaft
 $\bar{\quad}$: mean value
 θ : peripheral component

1. INTRODUCTION

Researches on system dynamics of a pump system have been performed (Barrand Ghelic and Caignaert 1993; Nguyen Kaenel and Danguy 1993; Rong Tanaka Tsukamoto and Tanaka 1996; Tsukamoto and Ohashi 1982; Rong Tanaka and Tsukamoto 1997). To analyze dynamic behaviors of a system equipped with fluid machinery, it is necessary to study dynamic characteristics especially in cavitating flow. These characteristics are traditionally obtained by performance tests. However, they cannot correctly represent the dynamic characteristics of turbomachinery, because:

1) The dynamic characteristics of turbomachinery systems are very complicated since these systems consist of mechanical, hydraulic and the other sub-systems. Especially the nonlinear characteristics are serious in a fluid sub-system. The sub-systems affect each other in a dynamic process;

2) As the behaviors of a turbomachinery system are combined with all sub-systems, it is difficult to distinguish the influence of them one by one.

Therefore, it is very useful to develop a mathematical model to express the dynamic characteristics of the fluid machinery, both in steady state and dynamic modes.

Bondgraphs method (Karnopp and Rosenberg 1990) has been used to solve the above problems recently (Paynter 1972; Rong Tanaka and Tsukamoto 1996). This is a method of analyzing system dynamics based on the conservation of energy flow within these systems. As this method modeling these systems is unified it is easy to derive the mathematical model of dynamic behaviors of the whole system including pump.

The mathematical model representing the dynamic behaviors of pump systems can predict the unsteady characteristics of the system. When the system operating point moves far from the design point as well as when cavitating flow occurs, the non-linear characteristics become more serious. Even in these cases, the Bondgraphs model can still represent the system dynamics correctly.

2. BONDGRAPHS OF THE PUMP SYSTEM

The schematic figure of a pump system in a closed circuit is illustrated in Fig. 1. In this paper, only the mechanical and hydraulic systems are considered to study the dynamic behaviors of the pump system. The power flow in this system is as follows;

The power from the motor is transferred to the pump shaft. A part of the shaft power is consumed through the mechanical and disk friction loss and the other are stored as the rotational inertia. The rest flows into the impeller, in which the mechanical power is converted into hydraulic power. In the process of conversion, there exist shock loss, friction loss and leakage loss. And also, in the dynamic mode, some of the power will be stored in the system acceleration as the liquid inertia in the impeller.

Then, the power flows into the volute casing where some of the kinetic energy will be converted into the pressure energy. In the process of conversion there also

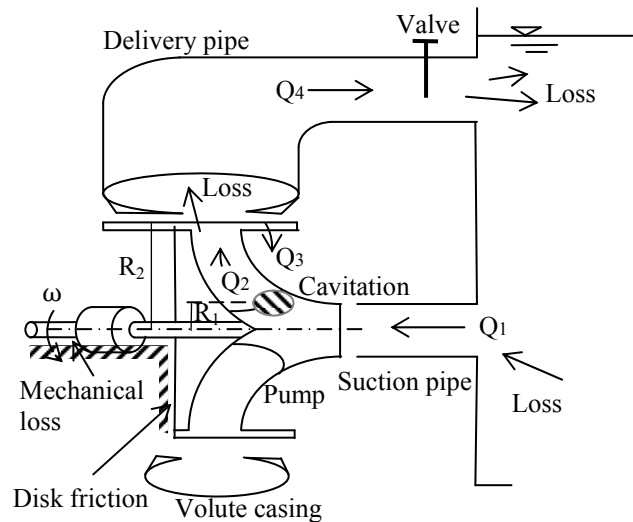


Figure 1: Pump system

exist shock loss and friction loss.

Then the power flows into the piping system, where there is friction loss. In the dynamic process, some of the power is stored due to the longitudinal acceleration of the liquid. The remaining power flows into the valve, some of which is consumed there.

Then the power flows into the tank with the expansion loss. Also when the power flows into the suction pipe from the tank, a part of the power will be consumed as the contraction loss as well as the friction loss. The remains flow into the pump. Here the power circulation closes in the pump system. The above power flow can be represented by using Bondgraphs, as shown in Fig. 2.

2.1. System Bondgraphs

In system Bondgraphs (Fig. 2), SE represents Torque input to the pump system through the rotating shaft of the motor system. The power input is $(T_0 \times \omega)$.

Before flowing into the impeller system, the power is divided into four components; the first is the power storing element I, $(\Delta T_I \times \omega)$ as the rotational inertia, the second is the power consuming element R_m , $(\Delta T_m \times \omega)$ as the mechanical loss and the third is the disk friction loss R_o , $(\Delta T_f \times \omega)$, and the last is transferred to the impeller.

In Bondgraphs, turbomachinery is represented as MGY element (Painter 1972). The mechanical power given to the impeller $[(T_0 - \Delta T_I - \Delta T_m - \Delta T_f) \times \omega]$ is converted to the fluid power $(P \times Q_2)$ by the test pump. The gyrating function of the MGY element is given as R_g (Rong Tanaka Tsukamoto and Tanaka 1996).

The power generated in the impeller $(P \times Q_2)$ separates into several components. The first of which is an element indicating fluid inertia in the impeller I_w , $(\Delta P_w \times Q_2)$. The second of which is R_{is} , $(\Delta P_{is} \times Q_2)$ element indicating hydraulic shock loss in the inlet of the impeller. The third of which is R_{if} , $(\Delta P_{if} \times Q_2)$ element indicating hydraulic loss in the impeller. And before the power flows into the volute casing, some power is consumed as leakage loss R_l , $\{(P_2 - P_1) \times Q_3\}$ because of the pressure difference between impeller inlet and outlet.

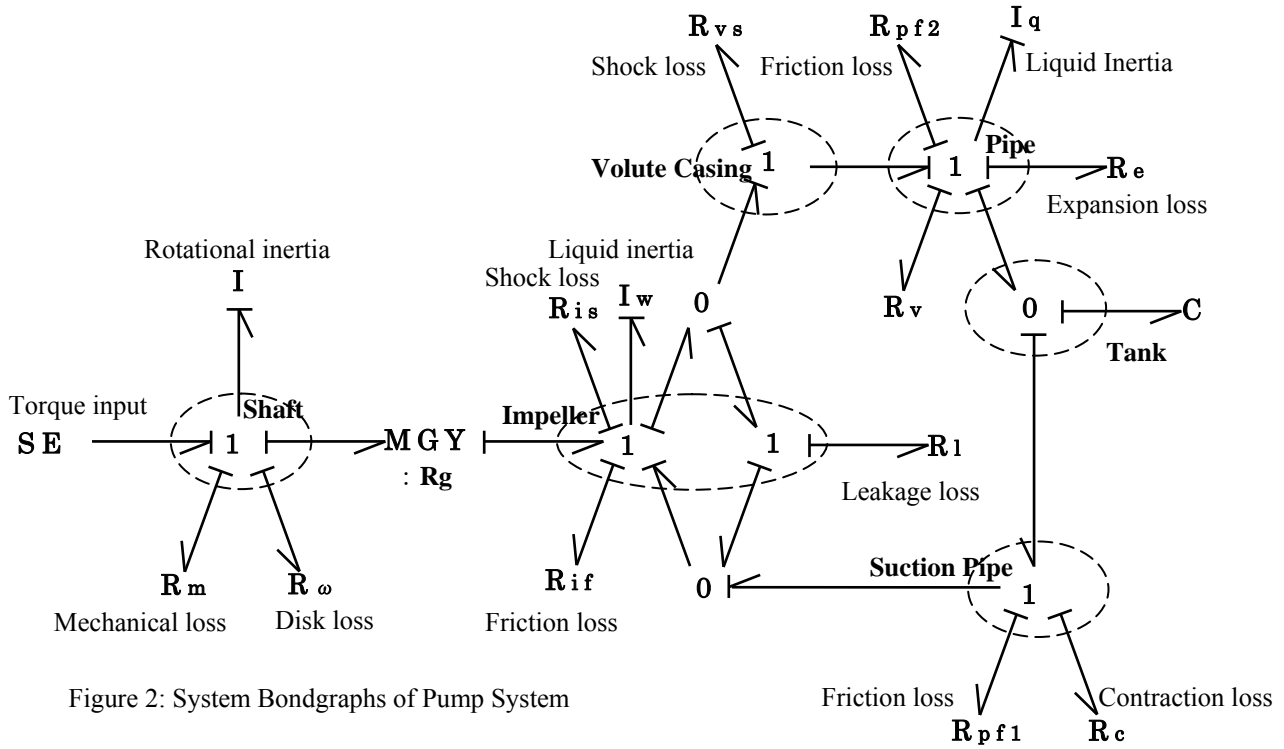


Figure 2: System Bondgraphs of Pump System

In the volute casing the hydraulic loss and shock loss are expressed as R_{vs} , $(\Delta P_{vs} \times Q_4)$ and R_{vf} , $(\Delta P_{vf} \times Q_4)$ elements respectively.

According to the modeling in a pipe and $P_4 = P_2 - \Delta P_{vs} - \Delta P_{vf}$, the power flows into the pipe $P_4 \times Q_4$ is divided into several power elements: hydraulic loss element R_{pf2} , $(\Delta P_{pf2} \times Q_4)$; energy storing element I_q , $(\Delta P_{Iq} \times Q_4)$ because of liquid inertia in the pipe and valve loss R_v , $(\Delta P_v \times Q_4)$; The remaining power $(P_4 - \Delta P_{pf2} - \Delta P_{Iq} - \Delta P_v) \times Q_4$ flows into the tank. Then power flows through the tank into the pipe only with losses. These are expansion loss R_e , $(\Delta P_e \times Q_4)$ and contraction loss R_c , $(\Delta P_c \times Q_4)$.

In case that the transients are very fast, the flow rate is much smaller than the water volume inside the tank, and even if cavitation phenomena are considered, the water level in the tank can be considered to be constant within the transients.

Then the power flows from the tank into the suction pipe. In the pipe, the power are divided into hydraulic loss R_{pf1} , $(\Delta P_{pf1} \times Q_1)$, inertia storing elements. And the remaining power flows into the impeller, $(P_1 \times Q_1)$. When cavitating flow happens at the impeller inlet, the phenomenon is represented by C_{cav} element. Then $Q_1 \neq Q_4$ because cavitation bubble occurs and its volume fluctuates. In non-cavitating flow, $Q_1 = Q_4$.

In the Bondgraphs, if an element is considered necessary or useful to represent the dynamic behaviors of a system, it can be added to the system Bondgraphs easily. On the other hand, if an element is considered to be negligible, it can be removed from the Bondgraphs. These corrections do not affect the computer program.

2.2. Mathematical Functions of Power Transfer Element in an Impeller

An impeller transfers rotational mechanical power to

hydraulic power. This power transformation can be represented as the following equation without losses.

$$T \cdot \omega = \rho [(uv_\theta)_2 - (uv_\theta)_1] Q_2 + (I_m + I_s + I_i) \frac{d\omega^2}{dt} + I_1 \frac{d\omega^2}{dt} - I_w \frac{dQ^2}{dt} \quad (1)$$

$$= \rho [(uv_\theta)_2 - (uv_\theta)_1] Q_2 + \Delta T_i \cdot \omega + \Delta T_i \cdot \omega - \Delta P \cdot Q_2$$

In this equation, T_0 is the input torque of the pump shaft. When $d\omega^2/dt=0$ and $dQ^2/dt=0$ in the steady mode, the equation becomes Euler equation of turbomachinery.

2.3. Losses in the system

There exist many losses in the process of power flow in the system. The main losses are shown as R elements in Fig. 2. The mathematical expressions of their representative losses are as follows according to JSME standard (1989).

2.3.1. Disk Friction Loss

Disk friction loss can be expressed in the following equation.

$$\Delta E_\omega = C_{M_D} D_2^5 N^3 \quad (2)$$

$$C_M = C_{M_D} + \sum C_{M_C} \quad (3)$$

ΔE_ω is energy loss in the disk friction loss and N is rotational speed of an impeller. The whole friction coefficient of an impeller is represented by Eq. (3), where C_{M_D} is coefficient on the disk, while C_{M_C} is friction coefficient on the peripheral area. C_{M_D} and C_{M_C}

can be calculated using the equations verified through experiments.

2.3.2. Friction loss in an impeller

The pressure loss based on the friction loss in an impeller can be expressed as

$$\Delta P_{I_f} = \xi_{I_f} (W_2^{*2} + W_1^{*2}) / 4 \quad (4)$$

W^* means relative velocity in case that slip factor is considered at the impeller outlet. ξ_{I_f} is a friction coefficient, which can be calculated using basic theory of fluid dynamics.

2.3.3. Shock Loss in an impeller

In general, the shock loss can be expressed as the following equation.

$$\Delta P_{I_s} = \xi_{I_s} (W_{u1} - W_{u1}^*)^2 / 2 \quad (5)$$

But this equation is effective only in the case of the rated operating point. When the system is operating in the other area or in the transient mode, this loss should be considered in detail.

The other losses such as leakage loss in the impeller, hydraulic and shock loss in the volute casing can be expressed using the same method. It should be noted here, in some cases of high speed transients cavitation will happen. This may affect the characteristics greatly. But in this research, the influence of cavitation to the dynamic behaviors are not considered

3. STATE SPACE EQUATION OF PUMP SYSTEM

Considering the system bondgraphs shown in Fig. 2, only one C element and three I elements, I , I_w and I_q , are time-dependent and the others are not. The following differential equations representing the dynamic behaviors of a pump system are obtained by eliminating all variables except the variable ω , Q_1 and Q_2 , from the characteristic functions of all elements derived in this paper and the algebraic equations for the conservation law at all junctions.

$$I' \frac{d\omega}{dt} = -R_m - R_\omega \omega^2 - R_g Q_2 + T_0$$

$$I' = I_s + I_i + I_m + I_l$$

$$I\omega \frac{dQ_2}{dt} = R_g \omega - (R_{i_s} R_{i_f}) Q_2^2 - R_l (Q_2 - Q_1)^2$$

$$I_{q1} \frac{dQ_1}{dt} + I_{q4} \frac{dQ_4}{dt} = R_l (Q_2 - Q_1)^2$$

$$-(R_{v_s} + R_{v_f} + R_v + R_e + R_{pf2}) Q_4^2 - (R_{pf1} + R_c) Q_1^2$$

$$R_g = \rho ((R_2^2 - R_1^2) \omega - \frac{Q_2}{2\pi} (\frac{1}{B_2 \tan \beta_2} - \frac{1}{B_1 \tan \beta_1})) \quad (7)$$

$$\beta_2 = \arctan\left(\frac{2\pi R_2^2 B_2 \omega \sqrt{\sin \beta_{b2}}}{Z^{0.7} Q_2} + \frac{1}{\tan \beta_{b2}}\right)^{-1} \quad (8)$$

Table 1: Parameters of Pump and Impeller (imp.)

Specific speed	$N_s \approx 130$ [rpm, m ³ /min, m]
Rated rotational speed	$N_r = 3455$ [rpm]
Rated head of pump	$H_r = 31.5$ [m]
Rated flow rate	$Q_r = 0.25$ [m ³ /min]
Rated efficiency	$\eta_r = 0.6$
Rated torque	$T_r = 5.925$ [N-m]
Rated input power	$P_r = 2.173$ [kW]
Imp. outlet diameter	$D_2 = 0.137$ [m]
Width in imp. outlet	$B_2 = 0.0093$ [m]
Thickness of blade at imp. inlet and outlet	$S_1 = 0.005$ [m] * $S_2 = 0.007$ [m] *
Blade angle at outlet	$\beta_{b2} = 20$ [°]
Diameter in imp. inlet	$D_1 = 0.07$ [m] *
Width in imp. inlet	$B_1 = 0.01$ [m] *
Blade angle at inlet	$\beta_{b1} = 15$ [°] *
Number of blades	7
Momentum	$0.012 + 0.0005$ [kg-m ²] *
	* Means estimated value

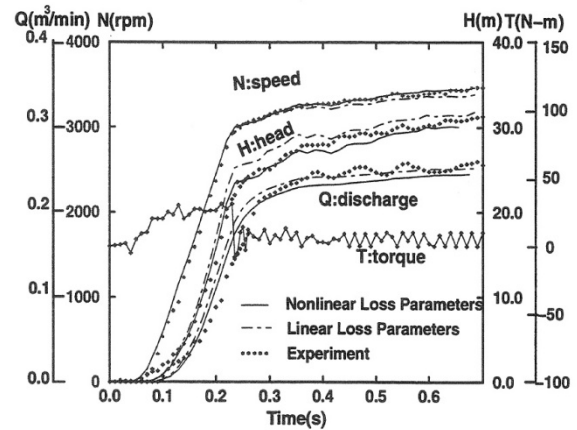


Figure 3: Dynamic behaviors of Pump Starting. Effects of Hydraulic Losses to Dynamics of Pump System

The system dynamic behaviors are decided by its own attributes, such as impeller diameter, blade angle and losses etc. In the cases with power input, the dynamic behaviors are decided by both system attributes and input T_0 .

4. SIMULATION RESULTS BASED ON SYSTEM BONDGRAPH

In the high speed starting modes of the test pump system, the total length of the pipes is $L_p = 5.1$ [m], while the diameter is $d_p = 0.05$ [m]. The other parameters of the system are listed in Table 1. In the high speed starting mode, the pump system is accelerated from stationary state to the rated state quickly. The results are shown in Fig. 3. In the simulation, the experimental data of torque was input to the system according to the experimental results.

In Fig. 3, we compare the simulation results with the experimental results. Even in the very fast starting mode, they agree very well. This means that system Bondgraphs shown in Fig. 2 and their mathematical model can represent the dynamic behaviors of systems equipped with turbomachinery.

From this comparison, we know that the losses have relatively little influence to the dynamic behaviors when the transients are very fast. In the case of constant loss parameters, parameters are calculated from the rated operating point. They are smaller than that in the nonlinear loss expressions. Because of this, the starting up in this case is a little faster than that in the case of nonlinear loss parameters. These results also affect the dynamic behaviors immediately after the starting up. However in the end of the process, the results of the two models will be the same, since in the steady state mode, their loss parameters are the same. From this comparison, Bondgraphs method is a useful method to represent the system.

5. CFD STUDY ON PUMP CAVITATING FLOW

5.1. Cavitation Analysis Method

Commercial CFD codes enable to analyze cavitation phenomena with good precision of numerical calculation recently (Philippe and Okamura 2002; Sato Nagahara Suzuki Tanaka Fuchiwaki, and Nishi 2009; Sato Nagahara Tanaka Fuchiwaki Shimizu and Inoue 2011). As solution methods for bubble flows, there are a VOF method of two-phase flow (Volume-of-Fluid Method), a cavity bubble tracking method and a method that solves the motion equation of Rayleigh-Plesset (Brennen 1995; Tamura Sugiyama and Matsumoto 2001; Tamura Fukaya and Matsumoto 2002) coupling it with flow equations to obtain fluid density mixed with water and bubbles. A method with the motion equation of Rayleigh-Plesset is used in this study. Its outline is shown below.

Usually, Eq. (9) of Rayleigh-Plesset for spherical bubbles is solved.

$$R \frac{d^2 R}{dt^2} + 3 \left(\frac{dR}{dt} \right)^2 = \frac{1}{\rho} \left(p_g - p - \frac{4\mu}{R} \frac{dR}{dt} - \frac{2\sigma}{R} \right) \quad (9)$$

Here, R indicates a radius of bubble, ρ liquid density, p_g gas pressure inside the bubble, p pressure of the liquid phase, μ viscosity coefficient of liquid phase and σ surface tension of liquid.

It is difficult to solve with multi-purpose software the detail of second order derivative term for approximation of the condition that bubbles repeat to grow and collapse with p_{in} , where vapour and air mixed. Therefore, it is common to solve the equations below. Equation (9) is simplified to Eq. (10) so that time variations of R are obtained.

< 1 > $p_g = p_v$; Bubbles are filled with saturated vapour continuously,

< 2 > Second order derivative term, surface tension term and viscous term are abbreviated.

$$\frac{dR}{dt} = \sqrt{\frac{2}{3} \frac{p_v - p}{\rho}} \quad (10)$$

In addition, when expressing void fractions α with R as a bubble radius and n_0 as number density per a unit volume of liquid,

$$\alpha = \frac{n_0 \frac{4}{3} \pi R^3}{1 + n_0 \frac{4}{3} \pi R^3} \quad (11)$$

Equation (12) is used as a transport equation of void fractions.

$$\frac{\partial \alpha}{\partial t} + \frac{\partial}{\partial x_j} (\alpha U_j) = \left(\frac{n_0}{1 + n_0 \frac{4}{3} \pi R^3} \right) \frac{d}{dt} \left(\frac{4}{3} \pi R^3 \right) \quad (12)$$

The equations mentioned above and the following conservation equation of mass and momentum (Navier-Stokes equation) are coupled and solved.

$$\frac{\partial \rho}{\partial t} + \frac{\partial}{\partial x_j} (\rho U_j) = 0 \quad (13)$$

$$\frac{\partial}{\partial t} (\rho U_j) + \frac{\partial}{\partial t} (\rho U_j U_i) = - \frac{\partial p}{\partial x_j} - \frac{\partial \tau_{ij}}{\partial x_j} + \rho f_j \quad (14)$$

5.2. Turbulence Model and Calculating Conditions

In prediction of pump oscillation in a test pump, cavitation occurrence with turbulence at the suction part is expected. Therefore, it is necessary to predict precisely the flow field at the suction part and the vortex occurrence caused by flow separation in particular. Transient rotor stator interface is used for the boundary between rotating part and stationary part. For a digitizing scheme, a second order upwind windward finite difference scheme is used for both convection and diffusion terms (Barth and Jespersen 1989). Simple method is used for an algorithm and inner iteration is assumed 50 iterations for each step. For boundary conditions, a pressure boundary and velocity integral boundary are used for the inlet and outlet, respectively.

Precision and reliability of capturing the sudden pressure rise after cavitation bubble collapse are compared among the results using a standard k- ϵ model, SST model and LES model in case that the number of grids is 5,200,000 elements. Overall features are almost the same in all cases though LES captures finer vortex structures such as the vorticity distributions at the location corresponding to the impeller inlet in each model. As a result, cavitating flow analyses have been performed with SST turbulence model from viewpoint of calculating conditions such as the number of grids, non-dimensional wall distance y^+ , and calculating time, as shown in Table 2. The calculation was performed every

Table 2: Calculating conditions

Details of elements	Number of elements	Maximum aspect ratio
Suction domain	437000 at $1.0 Q_0$ 548000 at $0.6 Q_0$	316.0
Impeller domain	557000	34.8
Volute domain	352000	309.3
Overall view	About 1400000	
N = 1800 rpm	z = 6 blades	y+ = 4 -150
$\Delta T = 9.26 \times 10^{-5}$ sec (for Impeller revolution by 1.0 degree)		SST turbulence model

time step correspondent to the impeller rotation by 1.0 degree, for 6 revolutions of the impeller.

5.3. Confirmation of Cavitation Occurrence

Figure 4 shows streamlines from the baffle plate to the rotational impeller. Rotational flow is generated near the baffle plate and the flow reaches the rotating impeller. There is a sign that the cavitation occurs from the baffle plate when there is strong rotation in the suction passage. In addition, there is one more sign that another cavitation occurs in the shroud side of the impeller. As a characteristic, this cavitation occurs from a low pressure region generated by leakage flow from the suction passage and mixed with main stream.

Figure 5 shows the iso-surface of $\alpha = 0.5$ of the vortex cavitation. The existence of the vortex cavitation from the baffle plate can be confirmed clearly in this figure. It can be seen that the vortex cavitation is generated near the baffle plate and reaches the rotating impeller. Hereafter, the impeller rotational angle shown in this figure becomes a norm, θ_0 .

5.4. Calculation of cavity volume

The commercial code can calculate the volume of cavities in each calculating domain. As there is a distribution of void fraction inside a cavity, air volume in the cavity is calculated from the product of volume-averaged void fraction in some calculating domain and the volume of the domain. Consequently, it becomes possible to calculate the air volume in each domain even when different type of cavitation occurs simultaneously in the different location.

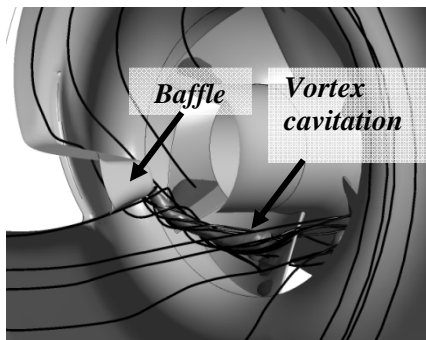


Figure 4: Stream lines and vortex cavitation from baffle plate (Simulation result, $\varphi=0.11$, $\sigma=0.30$)

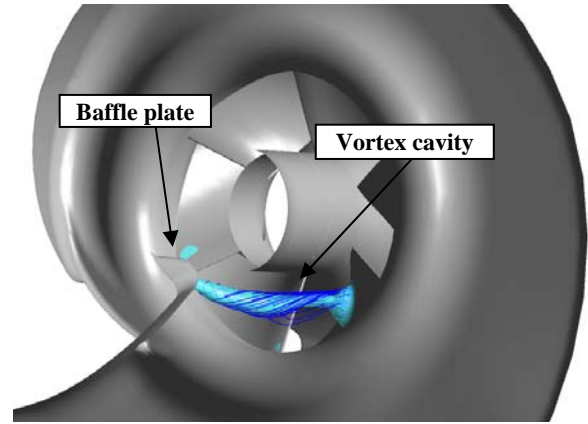


Figure 5: Iso-surface of $\alpha = 0.5$

6. SYSTEM MODEL OF CAVITATING FLOW

Cavitating flow raises many troubles, one of which is cavitation surge (Tsujiyama 2006; Yamamoto and Tsujiyama 2009). This is an important dynamic behavior of a pump system. Cavitation surge is considered as a complicated self oscillation phenomenon brought by total characteristics of the pump system. However, the surging frequency can easily be considered as the natural frequency of the pump system. Studies on the cavitation surge in a centrifugal pump have been performed under consideration that the phenomenon is supposed as quasi-linear self oscillation.

Here, basic characteristics of the surging frequency are analyzed one-dimensionally under quasi-steady response model using the CFD results on the cavitation surge in a centrifugal pump. In the field of pump cavitating flow, the characteristic parameters, cavitation compliance and mass flow gain factor, are generally used. Here, how to determine the value of the parameters is described.

6.1. Lumped parameter model of cavitation (C_p, M_b)

Assuming the quasi-steady response can be permitted in cavitating flows, cavitation volume can be represented by use of cavitation compliance C_p and mass flow gain factor M_b .

$$C_p = \frac{\partial V_c}{\partial P_1} \quad (15)$$

$$M_b = \frac{\partial V_c}{\partial Q_1} \quad (16)$$

$$\dot{V}_c = C_p \dot{P}_1 + M_b \dot{Q}_1 \quad (17)$$

Equation (17) can easily be replaced with an equation of spring-damper system in a mechanical system. Equation (17) is changed as follows.

$$P_1 = \frac{1}{C_p} \int \dot{V}_c dt - \frac{M_b}{C_p} Q_1 \quad (18)$$

Equation of continuity in Fig. 7,

$$\dot{V}_c = Q_1 + Q_3 - Q_2 = \Delta Q \quad (19)$$

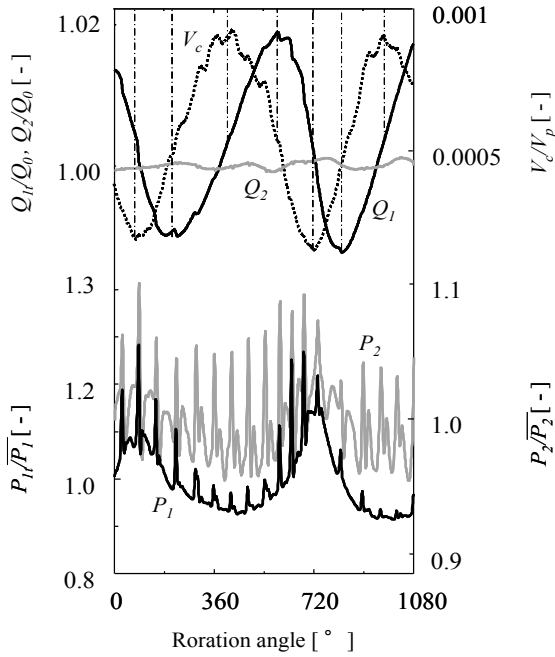


Figure 6: V_c - Q - P simulated by LES model ($\varphi=0.11$, $\sigma=0.30$)

From the above Eq. (17) and (18),

$$P_1 = \frac{1}{C_p} \int \Delta Q dt - \frac{M_b}{C_p} Q_1 \quad (20)$$

This is the characteristic equation of the cavitation element C_{cav} in Fig. 7.

This equation means that cavitating flow can be represented as spring-damper system. The spring coefficient is $1/C_p$ and damper coefficient is $-M_b/C_p$. In other words, a spring coefficient is defined as $-K/V_c$ in a lumped parameter system as follows.

$$\frac{1}{C_p} = -\frac{K}{V_c} = -\frac{\left(\frac{dp}{-dV_c/V_c}\right)}{V_c} = \frac{1}{dV_c/dp} \quad (21)$$

Because Eq. (21) is similar to Eq. (15), $1/C_p$ of Eq. (18) means the spring coefficient. Moreover, $-M_b/C_p$ of Eq. (18) is changed to the next equation.

$$-\frac{M_b}{C_p} = -\frac{\partial V_c / \partial Q}{\partial V_c / \partial P} = -\frac{\partial P}{\partial Q} \quad (22)$$

Because the last term means the gradient of pump performance curve, $-M_b/C_p$ indicates flow resistance coefficient of the pump system.

Figure 6 shows characteristics of cavitation compliance and mass flow gain factor. The phase of cavitation volume is quite opposite to suction pressure in the result. Therefore, the cavitation compliance is always negative from Eq. (15) and fluctuates according to the cavitation volume change from Eq. (21). Due to the phase difference between cavitation volume and suction flow rate, mass flow gain factor repeats positive and

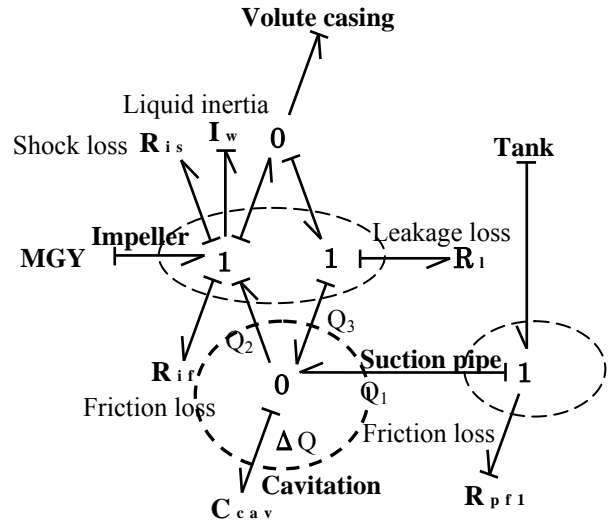


Figure 7: Bondgraphs Model of Cavitating Flow

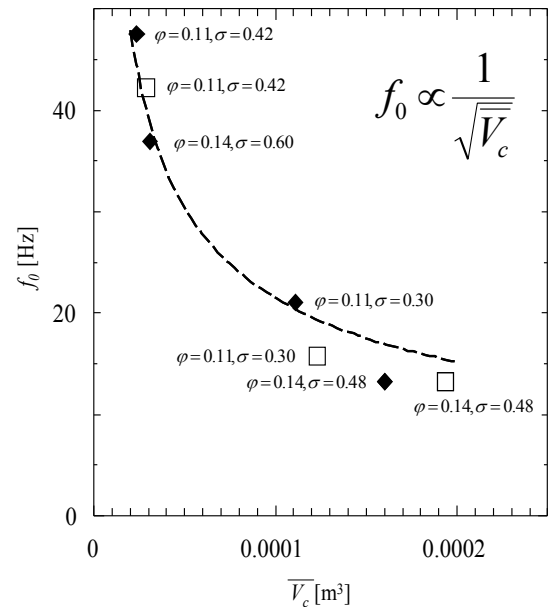


Figure 8: f_0 - \bar{V}_c simulated by SST model (\square), and by LES model (\blacklozenge), Approximate curve: $f_0 = 0.21/\sqrt{\bar{V}_c}$

negative values across the border indicated as the dashed line in Fig. 6 according to Eq. (16). When mass flow gain factor is negative, the pump system has negative resistance from Eq. (22). This means that pump performance has positive slope, which is clearly characteristic for negative damping of the system. These results show that cavitating flow system has two kind of self oscillation modes based on coefficient fluctuation and negative damping based on positive/negative fluctuation of flow resistance.

As stated above, cavitating flow in a pump can be represented by C element in Bondgraphs model as shown in Fig. 7 and the coefficient can be calculated by the cavity volume through CFD analysis. In the next section, the value of coefficient is validated by estimating natural frequency.

6.2. Natural frequency of pump system

Cavitation surge in a pump system can be modeled by considering a suction pipe and cavitation phenomenon. Here, the suction pipe is modeled by mass-damper system as represented in Eq. (19) and the cavitation phenomenon is modeled by spring-damper system as represented in Eq. (18). As a result, the pump system dynamics is represented by the following equations.

$$P_1 = -I_{q1} \dot{Q}_1 - R_1 Q_1 \quad (23)$$

$$I_{q1} \ddot{Q}_1 + \left(R_1 - \frac{M_b}{C_p} \right) \dot{Q}_1 - \frac{1}{C_p} Q_1 = \frac{-1}{C_p} Q_2 \quad (24)$$

From this equation, the natural frequency of pump system can be represented by the first and third terms.

$$f_0 = \frac{1}{2\pi} \sqrt{\frac{1}{-I_{q1} C_p}} \quad (25)$$

From Eq. (21) and Eq. (25),

$$f_0 = \frac{1}{2\pi} \sqrt{\frac{K}{I_{q1} V_c}} \quad (26)$$

In the above equation, $\overline{V_c}$ which is the mean value of V_c , can be replaced with V_c in Eq. (26) when cavitation volume V_c fluctuates.

$$f_0 = \frac{1}{2\pi} \sqrt{\frac{K}{I_{q1} V_c}} \quad (27)$$

CFD results on the cavitating flow are expressed by Eq. (27). Figure 8 shows the relationship between f_0 and $\sqrt{\overline{V_c}}$ and the approximate equation. This fact means that Bulk modulus can be assumed constant in the cavitation approximately.

Form the approximate equation in the Fig. 8, Bulk modulus is derived as follows.

$$\frac{1}{2\pi} \sqrt{\frac{K}{I_{q1}}} = 0.21 \quad \therefore K = 3.20 \times 10^4 [Pa] \quad (28)$$

Considering that Bulk modulus is $1.33 \times 10^5 [Pa]$ under normal condition, this value seems to be a little bit smaller.

However, if the vaporous pressure would be defined as $p = 3171 [Pa]$, the bulk modulus of pure vapor is calculated as the following, $K_{vapor} = \kappa p = 4.22 \times 10^3 [Pa]$.

The bulk modulus of water is $K_{water} = 2.06 \times 10^9 [Pa]$. The apparent bulk modulus of cavitation including water and pure vapor is defined as follows,

$$K_{cavi} = \frac{K_{water} K_{vapor}}{K_{vapor} + x(K_{water} - K_{vapor})} \quad (29)$$

where x means mixing ratio of water and vapor in a cavitating flow. The each value of K_{vapor} , K_{water} and K_{cavi} , that is given as $K = 3.20 \times 10^4 [Pa]$ in Eq. (28), is substituted into Eq. (29), the mixing ratio is calculated as $x = 13.2\%$. This value is considered as reasonable.

7. CONCLUSIONS

In this study, the Bondgraphs model representing the dynamic characteristics of a pump system has been used to perform modeling and simulation of the cavitating flow. As a result, the following conclusions are obtained.

- 1) Cavitating flow can be modeled by C element in Bondgraphs model.
- 2) The value of coefficient of the C element for cavitating flow can be calculated by CFD analysis.
- 3) Finally The system Bondgraphs of a pump system including cavitating flow has been established.

REFERENCES

- Barrand, J.P., Ghelici, N., and Caignaert, G., 1993. Unsteady flow during the fast start-up of a centrifugal pump, *ASME, FED-Vol. 154, Pumping Machine*, 143-150.
- Barth, T. J. and Jespersen, D. C., 1989. The Design and Application of Upwind Schemes on Unstructured Meshes, *AIAA Paper*, 89-0366.
- Brennen, C. E., 1995. *Cavitation and bubble dynamics*, Oxford University Press.
- Karnopp, D., Rosenberg, R., 1975. *SYSTEM DYNAMICS: A UNIFIED APPROACH*, John Wiley & Sons, Inc.
- JSME STANDARD, 1989. *Performance Conversion Method for Hydraulic Turbines and Pumps*.
- Nguyen Duc., J.M., Von Kaenel, A., and Danguy, F., 1993. Transient behaviors of liquid hydrogen pumps during start-up and shutdown of rocket engines, *ASME, FED-Vol. 154, Pumping Machinery*, 159-170.
- Painter, H.M., 1972. The Dynamics and Control of Eulerian Turbomachines, *Trans. ASME, Journal of Dynamic Systems, Measurement, and Control*, 198-205.
- Philippe, D. and Okamura, T., 2002. Cavitating Flow Calculations in Industry, *Proceedings of the 9th of International Symposium on Transport Phenomena and Dynamics of Rotating Machinery*, FD-146.
- Rong, W.H., Tanaka, K., Tsukamoto, H., Tanaka, H., 1996. Dynamic Behaviors Analysis of Pump System by Bond Graphs Method, *Proceeding of ASME FED-Vol. 237*, 805-812.
- Rong, W.H., Tanaka, K., Tsukamoto, H., 1997. Unsteady Characteristics and Transfer Matrix of Pump System based on Bondgraphs, *Proceeding of ASME FEDSM97-3368*, 1-7

- Sato, T., Nagahara, T., Suzuki, S., Tanaka, K., Fuchiwaki, M., and Nishi, M., 2009. Cavitation Analysis on Double-Suction Volute Pump, *Proceeding of 3rd IAHR International Meeting of the Workgroup on Cavitation and Dynamic Problems in hydraulic Machinery and Systems*, D1, 185-193.
- Sato, T., Nagahara, T., Tanaka, K., Fuchiwaki, M., Shimizu, F., and Inoue, A., 2011. Vortex Cavitation from Baffle Plate and Pump Vibration in a Double-Suction Volute Pump, *Int. Journal of Fluid Machinery and systems*, Vol. 4, No. 1, 76-83.
- Tsukamoto, H. and Ohashi, H., 1982. Transient Characteristics of a Centrifugal Pump During Starting Period, *Trans. ASME Journal of Fluids Engineering*, Vol. 104, 6-14.
- Tamura, Y., Fukaya, M., and Matsumoto, Y., 2002. Numerical Method for Cavitating Flow Simulations and Its Application to Axial Flow Pumps, *Proceedings of the 9th of International Symposium on Transport Phenomena and Dynamics of Rotating Machinery*, FD-129.
- Tamura, Y., Sugiyama, K., and Matsumoto, Y., 2001. Physical Modeling and Solution Algorithm for Cavitation Flow Simulations, *15th AIAA Computational Fluid Dynamics Conference*, AIAA2001-2652.
- Tsujimoto, Y., 2006. Flow Instabilities in Cavitating and Non-Cavitating Pumps, Design and Analysis of High Speed Pumps, RTO-EN-AVT-143, Paper 7, 7-1-7-24.
- Yamamoto, K. and Tsujimoto, Y., 2009. Backflow Vortex Cavitation and Its Effects on Cavitation Instabilities, *Int. Journal of Fluid Machinery and systems*, Vol. 2, No. 1, 40-54.

AUTHORS BIOGRAPHY

KAZUHIRO TANAKA,

He graduated from the University of Tokyo, obtained the first job as an assistant professor in Sophia University, and he moved back to the University of Tokyo. After then, he moved again to Kyushu Inst. of Tech. and is a professor. He has interests in CFD analyses on flow patterns inside components and systems as well as in analyses of dynamic characteristics for turbomachinery systems as well as oil-hydraulic systems.

TOSHIYUKI SATO

He graduated from Kyushu Inst. of Tech. as Ph.D student supervised by Prof. Tanaka. He is a high class engineer in Hitachi Ltd. for CFD analysis and design of turbomachinery including steady as well as unsteady flow. He has much interest in fishing.

HIROSHI TSUKAMOTO

He graduated from the University of Tokyo and moved to Kyushu Inst. of Tech. He retired as a professor of KIT and now the president of Kitakyushu National College of Japan. He has interests in transient characteristics of pump systems.

TAKEHISA KOHDA

He graduated from Kyoto University, obtained the first job in National Institute of Advanced Industrial Science and Technology, and moved back to Kyoto University. He is an associate professor. He developed BGSP, BondGraph Simulation Program, in Japan.

KATSUYA SUZUKI

He retired from Toyota Motor Corp., where he was a manager of Drive Train Division. He obtained Ph.D. degree in Nagoya University. He is now a visiting professor in Kyushu Inst. of Tech. and enjoys a lively discussion of Bondgraphs with Prof. Tanaka. He is a member of a chorus group singing the Ninth Symphony.